Supplementary Information

A mechanistic link between cellular trade-offs, gene expression and growth

Andrea Y. Weiße, Diego A. Oyarzún, Vincent Danos, Peter S. Swain

Contents

S1 Model definition

S1.1 Overview

We consider a mechanistic model of the cell. It combines nutrient import and its conversion to cellular energy with the biosynthetic processes of transcription and translation. In its basic form, the model includes 14 intracellular variables: internal nutrient s_i; energy, a, such as ATP[1]; and four types of proteins along with their corresponding free and ribosome-bound mRNAs. The four types of proteins we consider are (1) ribosomes r, (2) a transporter enzyme e_t and (3) a metabolic enzyme e_m, and (4) a class of house-keeping proteins q. We denote the corresponding free mRNAs by m_x and ribosome-bound mRNA by c_x with $x \in \{r, t, m, q\}$.

Table S1: List of reactions considered.

	dilution	transcription	dilution/degradation	ribosome binding	dilution	translation
ribosomes	$r \xrightarrow{\lambda} \varnothing$	$\varnothing \xrightarrow{\omega_r} m_r$	$m_r \xrightarrow{\lambda+d_m} \varnothing$	$r + m_r \underset{k_u}{\overset{k_b}{\leftrightarrow}} c_r$	$c_r \xrightarrow{\lambda} \varnothing$	$n_r\, a + c_r \xrightarrow{\nu_r} r + m_r + r$
transporter enzyme	$e_t \xrightarrow{\lambda} \varnothing$	$\varnothing \xrightarrow{\omega_t} m_t$	$m_t \xrightarrow{\lambda+d_m} \varnothing$	$r + m_t \underset{k_u}{\overset{k_b}{\leftrightarrow}} c_t$	$c_t \xrightarrow{\lambda} \varnothing$	$n_t\, a + c_t \xrightarrow{\nu_t} r + m_t + e_t$
metabolic enzyme	$e_m \xrightarrow{\lambda} \varnothing$	$\varnothing \xrightarrow{\omega_m} m_m$	$m_m \xrightarrow{\lambda+d_m} \varnothing$	$r + m_m \underset{k_u}{\overset{k_b}{\leftrightarrow}} c_m$	$c_m \xrightarrow{\lambda} \varnothing$	$n_m\, a + c_m \xrightarrow{\nu_m} r + m_m + e_m$
growth-independent proteins	$q \xrightarrow{\lambda} \varnothing$	$\varnothing \xrightarrow{\omega_q} m_q$	$m_q \xrightarrow{\lambda+d_m} \varnothing$	$r + m_q \underset{k_u}{\overset{k_b}{\leftrightarrow}} c_q$	$c_q \xrightarrow{\lambda} \varnothing$	$n_q\, a + c_q \xrightarrow{\nu_q} r + m_q + q$
internal nutrient	$s_i \xrightarrow{\lambda} \varnothing$	$s \xrightarrow{\nu_{\text{imp}}} s_i$	$s_i \xrightarrow{\nu_{\text{cat}}} n_s\, a$			
ATP	$a \xrightarrow{\lambda} \varnothing$	nutrient import	metabolism			

We model the cell as a system of ordinary differential equations derived from the

[1] Similarly a can also be interpreted as amino acids, or any other essential resource for biosynthetic reactions.

reactions listed in Table S1:

$$\dot{s}_i = \nu_{\text{imp}}(e_t, s) - \nu_{\text{cat}}(e_m, s_i) - \lambda s_i, \tag{1}$$

$$\dot{a} = n_s \cdot \nu_{\text{cat}}(e_m, s_i) - \sum_{\substack{x\in \\ \{r,t,m,q\}}} n_x \nu_x(c_x, a) - \lambda a, \tag{2}$$

$$\dot{r} = \nu_r(c_r, a) - \lambda r + \sum_{\substack{x\in \\ \{r,t,m,q\}}} (\nu_x(c_x, a) - k_b r m_x + k_u c_x), \tag{3}$$

$$\begin{aligned} \dot{e}_t &= \nu_t(c_t, a) - \lambda e_t, \\ \dot{e}_m &= \nu_m(c_m, a) - \lambda e_m, \\ \dot{q} &= \nu_q(c_q, a) - \lambda q, \end{aligned} \tag{4}$$

$$\dot{m}_x = \omega_x(a) - (\lambda + d_m) m_x + \nu_x(c_x, a) - k_b r m_x + k_u c_x, \tag{5}$$

$$\dot{c}_x = -\lambda c_x + k_b r m_x - k_u c_x - \nu_x(c_x, a), \qquad x \in \{r, t, m, q\}. \tag{6}$$

We consider all variables in molecules per cell. For the rates of those bimolecular reactions that depend on concentrations of molecular species, we assume a fixed volume of 1 μm^3 (approximately matching the volume of *E. coli*) to convert to numbers of molecules. The units of the parameters and their default values are listed in Table S2. The growth rate $\lambda = \lambda(\sum_x c_x, a)$ is a function of the number of translating ribosomes and energy. Below we elaborate on the main assumptions of the model and on the derivation of the reaction rates in Eqs. 1-6.

S1.2 Derivation of reaction rates

S1.2.1 Main assumptions

Apart from the three main trade-offs elaborated in the main text (finite energy, finite ribosomes and finite proteome) we base our model on the following assumptions:

1. First-order dilution of the intracellular species;
2. No degradation of proteins (although it can be included) and first-order degradation of mRNA;
3. Mass action kinetics for the binding and unbinding of mRNAs with free ribosomes;
4. Energy consumption within the cell is from translation only and we neglect the consumption from transcription [7, 8].

S1.2.2 Nutrient import and metabolism

We assume the enzymatically catalyzed reactions, nutrient import and metabolism, to be saturable and use Michaelis-Menten kinetics with maximal rates v_t and v_m and

Table S2: Model parameters. Default values were used unless otherwise stated. ★Obtained by parameter optimization (see §S3 for details). †Chosen relative to K_t; ‡chosen such that maximal growth rate matches that of *E. coli*; §*E. coli*'s average; ♯for steep auto-inhibition; *near the diffusion limit; ◇order of magnitude; aa denotes number of amino acids.

	description	default value	unit	source
s	external nutrient	10^4	[molecs]	†
d_m	mRNA-degradation rate	0.1	$[\text{min}^{-1}]$	[1]
n_s	nutrient efficiency	0.5	none	‡
n_r	ribosome length	7459	$[^{\text{aa}}/_{\text{molecs}}]$	[2]
n_x, $x \in \{t, m, q\}$	length of non-ribosomal proteins	300	$[^{\text{aa}}/_{\text{molecs}}]$	[3]§
$\gamma_{\max}$	max. transl. elongation rate	1260	$[^{\text{aa}}/_{\text{min molecs}}]$	[4]
K_γ	transl. elongation threshold	7	$[^{\text{molecs}}/_{\text{cell}}]$	★
v_t	max. nutrient import rate	726	$[\text{min}^{-1}]$	[5]
K_t	nutrient import threshold	1000	[molecs]	
v_m	max. enzymatic rate	5800	$[\text{min}^{-1}]$	[6]
K_m	enzymatic threshold	1000	$[^{\text{molecs}}/_{\text{cell}}]$	
w_r	max. ribosome transcription rate	930	$[^{\text{molecs}}/_{\text{min cell}}]$	★
$w_e = w_t = w_m$	max. enzyme transcription rate	4.14	$[^{\text{molecs}}/_{\text{min cell}}]$	★
w_q	max. q-transcription rate	948.93	$[^{\text{molecs}}/_{\text{min cell}}]$	★
θ_r	ribosome transcription threshold	426.87	$[^{\text{molecs}}/_{\text{cell}}]$	★
θ_{nr}	non-ribosomal transcription threshold	4.38	$[^{\text{molecs}}/_{\text{cell}}]$	★
K_q	q-autoinhibition threshold	152 219	$[^{\text{molecs}}/_{\text{cell}}]$	★
h_q	q-autoinhibition Hill coeff.	4	none	♯
k_b	mRNA-ribosome binding rate	1	$[^{\text{cell}}/_{\text{min molecs}}]$	*
k_u	mRNA-ribosome unbinding rate	1	$[\text{min}^{-1}]$	
M	total cell mass	10^8	[aa]	[4]◇
k_{cm}	chloramphenicol-binding rate	0.00599	$[(\text{min}\,\mu M)^{-1}]$	★

half-maximal thresholds K_t and K_m, such that

$$\nu_{\text{imp}}(e_t, s) = e_t \frac{v_t s}{K_t + s}, \qquad \nu_{\text{cat}}(e_m, s_i) = e_m \frac{v_m s_i}{K_m + s_i}. \tag{7}$$

In the basic cell model, we consider a constant environment, and so the external nutrient s is a constant parameter. In §S6 we show how to extend the basic model to include a dynamic environment. The nutrient efficiency parameter, n_s, determines energy yield per molecule of s_i.

S1.2.3 Translation

In exponentially growing microbes, protein synthesis, in particular translation-associated processes, accounts for a major part of the energy budget [7, 8, 9]. Here we assume a simplified mechanism, illustrated in Fig. S1, to derive the dependence of the translation rates on the energy levels of the cell. Using the rate constants in Fig. S1 and defining

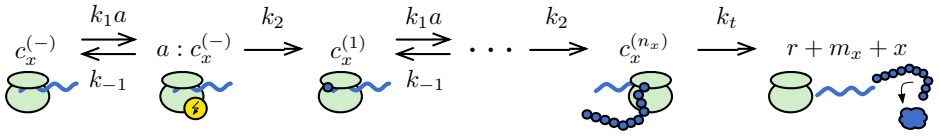

Figure S1: A simplified mechanism of translation. In a reversible reaction, the mRNA-ribosome complex, c_x, binds energy. In a second step, the nascent peptide chain elongates by one amino acid consuming energy. The two steps are repeated n_x times, where n_x is the length in amino acids of protein x. Finally, termination of translation releases the ribosome, the mRNA and the newly synthesised protein.

$K_p := \frac{k_1 k_2}{k_{-1}+k_2}$, we can derive the net rate [10] of translating a protein x as

$$\nu_x(c_x, a) = c_x \left(n_x \left(\frac{1}{K_p a} + \frac{1}{k_2} \right) + \frac{1}{k_t} \right)^{-1}. \tag{8}$$

Assuming that the final termination step is fast, $\frac{1}{k_t} \ll n_x \left(\frac{1}{K_p a} + \frac{1}{k_2} \right)$, we write ν_x as

$$\nu_x(c_x, a) \approx c_x \frac{\gamma(a)}{n_x}, \qquad \gamma(a) := \frac{\gamma_{\max} a}{K_\gamma + a}, \tag{9}$$

where n_x is the length of protein x (in amino acids) and γ is the rate of translational elongation with maximal rate $\gamma_{\max} = k_2$ and threshold $K_\gamma = {}^{k_2}/_{K_p}$ for half-maximal elongation.

S1.2.4 Transcription

The contribution of transcription-associated processes to the overall consumption of energy is small compared to that of translation (less than 10% in rapidly growing *E. coli* and *S. cerevisiae* [7, 8]), and so we neglect this contribution to energy consumption.

We do, however, let transcription be an energy-dependent process that ceases when the cell runs out of energy. Analogous to translation (see Fig. S1), transcription involves repeated steps of elongation that each depend on energy. If we assume that the energy consumed in each elongation step is constant, it follows that the effective transcription rate has the form

$$\omega_x(a) = w_x \frac{a}{\theta_x + a}, \qquad x \in \{r, t, m\}. \tag{10}$$

Unlike the translational elongation thresholds, the transcriptional thresholds θ_x depend on the gene x. We distinguish two transcriptional thresholds, $\theta_x = \theta_{\text{nr}}$ for all non-ribosomal genes $x \in \{t, m, q\}$ and $\theta_r \neq \theta_{\text{nr}}$ for ribosomal genes, because ribosomal expression may have a different sensitivity to physiological changes within the cell. The maximal rate of transcription, w_x, is a lumped description of the speed of transcriptional elongation and gene-related information such as copy number, induction and length. We assume that the transporter and the metabolic enzymes, e_t and e_m, are co-expressed and so $w_t = w_m = w_e$.

We further assume that all but the q-proteins have a transcription rate that solely depends on energy levels. The q-proteins, we assume, are auto-regulated to sustain stable protein levels across different growth conditions. Following [11], we thus model the effective rate of q-transcription by

$$\omega_q(q, a) = w_q \frac{a}{\theta_x + a} \mathcal{I}(q), \quad \text{with} \quad \mathcal{I}(q) := \frac{1}{1 + (q/K_q)^{h_q}}, \tag{11}$$

where $\mathcal{I}$ is the auto-inhibition function with threshold K_q and Hill-coefficient h_q.

S1.2.5 Growth and dilution

The growth rate λ is crucial to connect the cellular processes with growth, as it dilutes all intracellular species by redistributing the cellular content between mother and daughter cells (Table S1). We define the total mass of the cell as the total protein mass (including bound ribosomes):

$$M = \sum_x n_x x + n_r \sum_x c_x. \tag{12}$$

Defining the number of translating ribosomes $\sum_x c_x$ to be R_t, we can show that

$$\frac{dM}{dt} = \gamma(a) R_t - \lambda M. \tag{13}$$

At steady-state, the growth rate

$$\lambda = \frac{\gamma(a) R_t}{M}, \tag{14}$$

is therefore proportional to the rate of protein synthesis, which agrees with other definitions of growth rate in the literature [12, 13, 14]. Here M is the the mass of a mid-log cell.

We emphasize that specifying a value for M at steady-state (M_s), the typical mass in numbers of amino acids of the proteins of a mid-log cell, is necessary to fully parameterize our model and by doing so we impose the constraint Eq. 12, and so the trade-off in levels of proteins. For the simulations, we assume that Eq. (14), with $M = M_s$, also holds away from steady-state.

S1.3 SBML representation

Versions of the model in SBML, Matlab, and in the Facile format [15] are available at `swainlab.bio.ed.ac.uk`.

S2 Bacterial growth laws

The phenomena recently termed 'bacterial growth laws' are empirical relations between the growth rate and the ribosomal mass fraction of exponentially growing cells [14] and Monod's law, which states a Michaelis-Menten-type relation between growth rate and extracellular nutrient [16]. Previous work used phenomenological models to explain the growth laws [13, 17]. Here we derive the bacterial growth laws from our mechanistic model (an alternative derivation is also given by Scott *et al.* [18]).

S2.1 The first law

The total amount of ribosomes obeys

$$R = r + R_t \tag{15}$$

with r being the amount of free ribosomes. If we assume that Eq. (14) holds generally, then as in [13]:

$$\lambda = \frac{1}{\tau_\gamma}\left(\phi_R - \phi_r\right), \tag{16}$$

with the mass fractions $\phi_R = n_r R/M$ and $\phi_r = n_r r/M$, and $\tau_\gamma = {}^{n_r}/_{\gamma}$ denotes the ribosome synthesis time, that is, the time it takes to translate one ribosome and is a measure of ribosome efficiency. Eq. 16 corresponds to the first growth law if τ_γ is approximately constant (for example, when the elongation rate $\gamma(a)$ is near saturation). Our choice of ω_t and ω_r in Eq. 10 ($\theta_r \gg \theta_{\mathrm{nr}}$) ensures that the mass fraction of ribosomes increases for better quality media (modelled as a larger n_s).

S2.2 The second law

S2.2.1 Balancing energy fluxes

Consider the equation for cellular energy

$$\frac{da}{dt} = n_s e_m \frac{v_m s_i}{K_m + s_i} - \gamma R_t - \lambda a. \tag{17}$$

Then, at steady-state,

$$\lambda \frac{a}{M} + \lambda = \frac{\phi_m}{n_m} \frac{v_m s_i}{K_m + s_i}, \tag{18}$$

using Eq. (14) and dividing through by the mass M, where $\phi_m = n_m e_m / M$. We define the metabolic synthesis time $\tau_m = {}^{n_m}/_{n_s v_m}$, the minimal time taken by an enzyme to generate sufficient energy to synthesize a new metabolic enzyme, as a measure of metabolic efficiency. Assuming $a \ll M$ at steady-state, then Eq. (18) becomes

$$\lambda \approx \frac{\phi_m}{\tau_m} \frac{s_i}{K_m + s_i}, \tag{19}$$

and relates growth rate to the mass fraction of a 'bottleneck' metabolic enzyme, ϕ_m [13].

We can also consider the differential equation for internal nutrient:

$$\frac{ds_i}{dt} = e_t \frac{v_t s}{K_m + s} - e_m \frac{v_m s_i}{K_m + s_i} - \lambda s_i \tag{20}$$

at steady-state. Setting $\frac{ds_i}{dt} = 0$ and dividing through by M, then we find that

$$\frac{\phi_t}{\tau_t} \frac{s}{K_t + s} = \frac{\phi_m}{\tau_m} \frac{s_i}{K_m + s_i} + \lambda \frac{n_s s_i}{M}, \tag{21}$$

where we defined the transporter synthesis time $\tau_t = {}^{n_t}/_{n_s v_t}$, in analogy to the metabolic synthesis time τ_m, to be the minimal time taken by a transporter to import sufficient nutrient to make another transporter (a measure of the efficiency of transport), and wrote the transporter mass fraction as $\phi_t = n_t e_t / M$. If the steady-state cellular consumption of s_i is larger than the loss of s_i through dilution (the first term outweighs the second term in the right hand side of Eq. 21), then the rate of import of the nutrient approximately matches its rate of metabolism:

$$\frac{\phi_t}{\tau_t} \frac{s}{K_t + s} \approx \frac{\phi_m}{\tau_m} \frac{s_i}{K_m + s_i}. \tag{22}$$

Eqs. 19 and 22 then imply that

$$\frac{\phi_t}{\tau_t} \frac{s}{K_t + s} \approx \lambda, \tag{23}$$

which relates the growth rate to the mass fraction of a 'bottleneck' transporter.

S2.2.2 Determining ratios of enzymes

By solving the steady-state equations for m_x, c_x, and e_x, we find that

$$e_x = \frac{\frac{\gamma k_b \omega_x r}{\lambda n_x}}{(d_m + \lambda)\left(\frac{\gamma}{n_x} + k_u + \lambda\right) + \lambda k_b r}, \tag{24}$$

and consequently that

$$\frac{e_m}{e_t} \approx \frac{n_t \omega_m}{n_m \omega_t} \tag{25}$$

if either $n_m \approx n_t$ or $\gamma/n_x \ll k_u + \lambda$ for both enzymes. Eq. 25 implies that the mass fractions are approximately given by the ratio of transcription rates

$$\frac{\phi_m}{\phi_t} \approx \frac{\omega_m}{\omega_t}. \tag{26}$$

If the dependencies of the two transcription rates on energy are approximately equal (i.e. $w_m \approx w_t$), then Eq. (26) implies that the ratio of mass fractions is approximately constant.

S2.2.3 Deriving the second law

Using Eqs. (19) and (23) in the equation for the conservation of mass

$$\phi_m + \phi_t + \phi_R = 1 - \phi_q, \tag{27}$$

we find

$$\phi_R \approx 1 - \phi_q - \lambda \left[\frac{K_m + s_i}{s_i} \tau_m + \frac{K_t + s}{s} \tau_t \right]. \tag{28}$$

From Eqs. (22) and (26),

$$\frac{\tau_m}{\tau_t} = \frac{\omega_m}{\omega_t} \frac{K_t + s}{s} \frac{s_i}{K_m + s_i} \tag{29}$$

and Eq. (28) then becomes

$$\phi_R \approx 1 - \phi_q - \lambda \frac{K_t + s}{s} \tau_t \left[\frac{\omega_m}{\omega_t} + 1 \right]. \tag{30}$$

Writing $\tau_e = \tau_t(1 + {}^{w_m}/_{w_t})$ to denote the enzyme synthesis time, which is the minimal time taken to import sufficient nutrient to synthesize both a transporter and a metabolic enzyme, then Eq. (30) becomes

$$\phi_R \approx 1 - \phi_q - \lambda \frac{K_t + s}{s} \tau_e, \tag{31}$$

which is the second law (Eq. 12 in the main text). Note that the second law was shown to hold empirically in constant media, that is for a constant s [13]. We have assumed that the rates of transcription of the two enzymes have a similar energy dependence so that ${}^{\omega_m}/_{\omega_t}$ is a constant. Note further that the enzyme synthesis time scales with the inverse of the nutrient efficiency, $\tau_e \sim 1/n_s$, explaining the slopes obtained in the translation inhibition experiments for varying nutrient conditions (Fig. 1B).

S2.3 Monod's law

Using Eqs. (16), (19) and (23) in the equation for conservation of mass, Eq. (27), gives

$$\lambda \left[\frac{K_t + s}{s} \cdot \tau_e + \tau_\gamma \right] + \phi_r \approx 1 - \phi_q, \tag{32}$$

or

$$\lambda \approx \frac{1 - \phi_q - \phi_r}{\frac{K_t+s}{s}\tau_e + \tau_\gamma}. \tag{33}$$

Finally, if $\phi_r \ll \phi_q$ then

$$\lambda \approx \frac{(1 - \phi_q)s}{K_t\tau_e + (\tau_e + \tau_\gamma)s}. \tag{34}$$

Changing the extracellular amount of nutrient can cause the ribosome synthesis time τ_γ to vary with levels of energy. Eq. (34) therefore is Monod's law if either (i) the steady-state synthesis time τ_γ is approximately constant across different nutrient conditions (and so the translation elongation rate γ is approximately constant), or (ii) enzyme activity is growth-limiting so that

$$\frac{K_t + s}{s}\tau_e \gg \tau_\gamma. \tag{35}$$

Note that the enzyme synthesis time τ_e depends on the inverse of the nutrient efficiency, and so for varying nutrient conditions Eq. (34) saturates with increasing nutrient efficiency n_s:

$$\lambda \approx \frac{(1 - \phi_q)sn_s}{(K_t + s)\frac{n_t}{v_t}\left(1 + \frac{\omega_m}{\omega_t}\right) + s\tau_\gamma n_s}, \tag{36}$$

where we have used the definitions of the synthesis times τ_e and τ_t. To summarize, Monod growth follows from our model if either translational elongation is stable across different nutrient media (saturated, for example) or if enzyme activity is growth limiting.

Additional to the common relation between growth rate and nutrient abundance, the mechanistic derivation of Monod's law, Eq. (34), highlights the dependence on some experimentally accessible quantities: the nutrient, enzyme and ribosome efficiencies, and the load of house-keeping genes.

S2.4 The importance of the trade-offs

Our model is based around three fundamental trade-offs faced by all growing cells, but it is possible that the growth laws can be derived from an alternative model with fewer trade-offs. Central to our derivation, and necessary for all three laws, is the assumption of a finite proteome because this trade-off, Eq. 12, allows us to derive Eq. 14 and so the first growth law (Eq. 16). Further, Eq. 12 relates the mass fraction of ribosomes and so growth rate, via Eq. 14, to the mass fraction of other proteins. Similarly,

the trade-off in energy allows growth rate to be related to the levels of the metabolic enzyme (Eq. 19). Consequently, this trade-off is necessary for the derivation of the second law (Eq. 31) and Monod's law (Eq. 34). The trade-off in ribosomes, however, appears less important and contributes (mathematically) the non-zero intercept to the first growth law (the ϕ_r term in Eq. 16). Nevertheless, the trade-off in ribosomes, and that $\theta_r \gg \theta_{\rm nr}$, ensures that the mass fraction of ribosomes, ϕ_R, increases as the experimentally accessible parameter, n_s (a measure of the quality of the growth media), is increased. Eq. 14 then causes the growth rate to increase too, as expected.

S2.5 The impact of gratuitous proteins on growth rate

If the cell expresses a gratuitous protein p (that does not contribute to growth), then analogous to the derivation of Eq. (33) we find that

$$\phi_p \approx 1 - \phi_q - \phi_r - \lambda \left[\frac{K_t + s}{s} \tau_e + \tau_\gamma \right]. \tag{37}$$

If $\phi_r \ll \phi_q$ and if translation is growth-limiting, that is,

$$\frac{K_t + s}{s} \tau_e \ll \tau_\gamma, \tag{38}$$

then

$$\phi_p \approx 1 - \phi_q - \tau_\gamma \lambda \tag{39}$$

or

$$\lambda \approx \frac{1}{\tau_\gamma} \left(1 - \phi_q - \phi_p\right) \tag{40}$$

in analogy to the first law, Eq. (16), and in agreement with data from [13].

S3 Parameter optimization, sensitivity and sloppiness

S3.1 Including translational inhibition

To fit the data from [13], we considered a mechanism in which chloramphenicol, c_m, binds the mRNA-ribosome complexes, forming a 'zombie'-complex $\overline{zm}_x$, which is no longer available to translation. We assume that the chloramphenicol concentration in the cell remains constant, i.e. c_m is not consumed. Altogether, for each protein-type $x \in \{r, t, m, q\}$, we add a binding and a dilution reaction:

$$\begin{aligned} c_x &\xrightarrow{c_m \cdot k_{\rm cm}} \overline{zm}_x, \\ \overline{zm}_x &\xrightarrow{\lambda} \varnothing. \end{aligned} \tag{41}$$

The rate constant $k_{\rm cm}$ includes the conversion from the concentrations applied in [13] to molecule numbers and was fit as described below. To account for the extra reactions

(41), we include equations for the chloramphenicol complexes and modify the equations of mRNA-ribosome complexes:

$$\dot{\overline{zm}}_x = c_x c_m k_{\rm cm} - \lambda \overline{zm}_x, \tag{42}$$

$$\dot{c}_x = -\lambda c_x + k_b r m_x - k_u c_x - \nu_x(c_x, a) \quad - \quad c_x c_m k_{\rm cm} \tag{43}$$

for $x \in \{r, t, m, q\}$ and with blue marking the modification to the original equations (6).

S3.2 Parameter optimization

We fit the growth rate and the ribosomal mass fractions to data with translational inhibition (strain EQ2, columns 1 & 2 of Table S2 in [13]). We use the experimental chloramphenicol concentrations, $c_m \in \{0, 2, 4, 8, 12\}$ μM and model the different nutrient conditions by varying the nutrient efficiency, choosing n_s as six equally log-spaced points between $n_s = 0.08$ and $n_s = 0.5$.

The parameters included in the estimation were the maximal transcription rates w_x, $x \in \{r, e, q\}$, the transcriptional energy-thresholds θ_r and $\theta_{\rm nr}$, the translational energy-threshold, K_γ (through fitting $K_p = \gamma_{\rm max}/K_\gamma$), the auto-inhibition threshold K_q, and the chloramphenicol binding rate constant $k_{\rm cm}$. We estimated the eight parameters in a Bayesian fashion, using an adaptive Monte Carlo Markov chain method [19] to sample the posterior probability distribution for the parameters. The final estimates given in Table S2 are the modes of the resulting marginal posterior distributions.

S3.3 Sensitivity and sloppiness

From the posterior distribution, we estimated the Fisher information matrix (FIM) by the pseudo-inverse of the variance-covariance matrix [20]. The eigenvalues of the FIM spread over orders of magnitude (Fig. S2A), indicating that the model is 'sloppy' [21, 22] and the parameters are not fine-tuned. Indeed, computing the parameter sensitivities from the FIM [20], we find that most parameters have low sensitivities (Fig. S2B). An exception is the maximal enzyme transcription rate, w_e, showing high sensitivity, because fixing the nutrient efficiencies, n_s, for the different experiments constrains the value of w_e.

S3.4 Discussion

To fit the data we had to quantify the quality of the growth media chosen by Scott *et al.* In the model, the growth media are represented by the single parameter n_s, but Scott *et al.* varied their media in multiple ways including the sources of carbon, nitrogen and amino acids [13]. We thus had to make a choice of how to quantify these differences with one parameter (S3.2). The posterior values of the parameters generate a good fit with the data obtained in poor nutrient conditions (Fig. 1B). The weaker fit for the two richest conditions (green lines) is, however, an artefact of our choices for n_s. An alternative is to fit the values of n_s too, but we found this approach led to overfitting because of the small number of data points. We suggest refitting the model

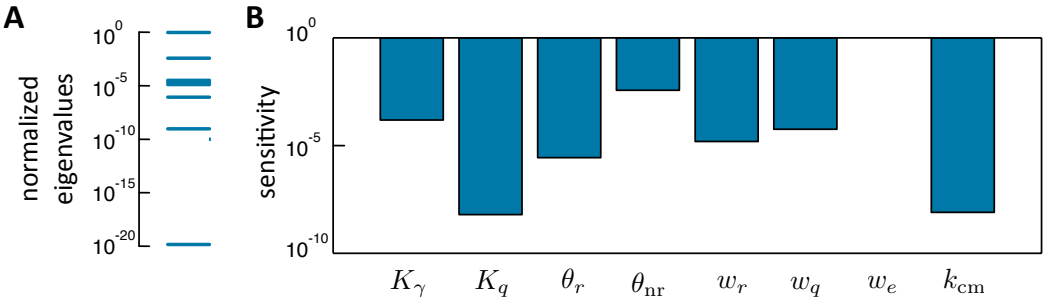

Figure S2: Fisher information. A The eigenvalues of the Fisher information matrix, normalized by the largest eigenvalue, spread over several orders of magnitude. B Parameter sensitivity with values close to one indicate that the model fit is sensitive to changes in the parameter.

to a data set where the difference in growth media is determined by varying a single parameter, such as the concentration of a limiting nutrient.

S4 Dosage compensation

S4.1 Modelling paralog deletion

To model the deletion of a duplicate of the gene for an enzyme, we halve the maximal enzyme transcription rate in the deletion strain compared to the wild-type transcription rate: $w_e^{\Delta_e} = {}^{w_e}/_2$.

To model the expression of a gratuitous protein, denoted p, we included three new species, the protein itself and its free and ribosome-bound mRNA forms, m_p and c_p, introducing equations, equivalent to Eqs. (4)–(6), for each:

$$\dot{p} = \nu_p(c_p, a) - \lambda \cdot p, \tag{44}$$

$$\dot{m}_p = \omega_p(a) - (\lambda + d_m)m_p + \nu_p(c_p, a) - k_b r m_p + k_u c_p, \tag{45}$$

$$\dot{c}_p = -\lambda c_p + k_b r m_p - k_u c_p - \nu_x(c_p, a). \tag{46}$$

We include the additional consumption of energy and ribosomes by

$$\begin{aligned} \dot{a} &= n_s \nu_{\mathrm{cat}}(e_m, s_i) - \lambda a - \sum_{\substack{x \in \\ \{r,t,m,q\}}} n_x \nu_x(c_x, a) \quad -n_p \nu_p(c_p, a), \\ \dot{r} &= \nu_r(c_r, a) - \lambda r + \sum_{\substack{x \in \\ \{r,t,m,q\}}} (\nu_x(c_x, a) - k_b r m_x + k_u c_x) \\ &\quad +(\nu_p(c_p, a) - k_b r m_p + k_u c_p), \end{aligned} \tag{47}$$

where blue marks the changes to the original Eqs. (2) & (3). Further, we modify the

growth rate, (14) to include p-synthesis:

$$\lambda = \frac{\gamma(a)}{M}\left(\sum_{\substack{x\in\\ \{r,t,ms,q\}}} c_x + c_p\right). \tag{48}$$

We chose the maximal wild-type transcription rate equal to the transcription rate of the enzymes, $w_p = w_e$, and set $w_p^{\Delta_p} = w_p/2$ for the Δ_p-strain. To see responsiveness of the same order of magnitude as in the Δ_e-strain, we had to set maximal wild-type transcription for p-protein to ten times that of the enzymes, $w_p = 10w_e$.

S4.2 Responsiveness

We computed the responsiveness comparing the steady-state protein levels x of the deletion, $\Delta_y,\ y \in \{e, p\}$, and the wild-type strains by [23]

$$R(x) = \log_2\left(\frac{x^{\Delta_y}}{\delta(x,y)\cdot x^{\mathrm{wt}}}\right), \qquad \delta(x,y) := \begin{cases} 1, & x \neq y \\ 0.5, & x = y \end{cases}, \tag{49}$$

where $\delta(x, y)$ ensures that we compare the expression of the remaining duplicate gene in the deletion strain with the expression of only one of the duplicate genes in the wild-type strain.

For each strain we compute the relative transcription rate of mRNA of type x by

$$P(x) = \frac{\omega_x(a)}{\sum_y \omega_y(a)}, \tag{50}$$

as a measure of its ability to compete for ribosomes. We compare the relative transcription rates in the deletion strains $P_{\Delta_x}(\mathrm{nr}),\ x \in \{e, p\}$ with those in the wild-type strains $P_{\mathrm{wt}}(nr)$ in Fig. 2d.

S5 Synthetic gene circuit

S5.1 A host-aware model of the repressilator

We adapted the repressilator model from [24]. The repressilator-host model contains nine additional species compared to the original cell model: three mRNAs (m_{g1}, m_{g2} and m_{g3}), their three ribosomal complexes (c_{g1}, c_{g2} and c_{g3}), and the three proteins (g_1, g_2 and g_3). Theses species are involved in the reactions of Table S3 and lead to the differential equations:

$$\begin{aligned} \dot{g}_i &= \nu_{gi}(c_{gi}, a) - (\lambda + d_g)g_i, \\ \dot{m}_{gi} &= \omega_{gi}(g_{i-1}, a) - (\lambda + d_{m,g})m_{gi} + \nu_{gi}(c_{gi}, a) - k_b r m_{gi} + k_u c_{gi}, \\ \dot{c}_{gi} &= -\lambda c_{gi} + k_b r m_{gi} - k_u c_{gi} - \nu_{gi}(c_{go}, a), \qquad i = \{1, 2, 3\}, \end{aligned} \tag{51}$$

Table S3: List of additional reactions in the repressilator-chassis model.

	dilution/degr.	transcription	dilution/degradation	ribosome binding	translation
repressor 1	$g_1 \xrightarrow{\lambda+d_g} \varnothing$	$\varnothing \xrightarrow{\omega_{g1}} m_{g1}$	$m_{g1} \xrightarrow{\lambda+d_{m,g}} \varnothing$	$r + m_{g1} \overset{k_b,\,k_u}{\longleftrightarrow} c_{g1}$	$n_g\, a + c_{g1} \xrightarrow{\nu_{g1}} r + m_{g1} + g_1$
repressor 2	$g_2 \xrightarrow{\lambda+d_g} \varnothing$	$\varnothing \xrightarrow{\omega_{g2}} m_{g2}$	$m_{g2} \xrightarrow{\lambda+d_{m,g}} \varnothing$	$r + m_{g2} \overset{k_b,\,k_u}{\longleftrightarrow} c_{g2}$	$n_g\, a + c_{g2} \xrightarrow{\nu_{g2}} r + m_{g2} + g_2$
repressor 3	$g_3 \xrightarrow{\lambda+d_g} \varnothing$	$\varnothing \xrightarrow{\omega_{g3}} m_{g3}$	$m_{g3} \xrightarrow{\lambda+d_{m,g}} \varnothing$	$r + m_{g3} \overset{k_b,\,k_u}{\longleftrightarrow} c_{g3}$	$n_g\, a + c_{g3} \xrightarrow{\nu_{g3}} r + m_{g3} + g_3$

with $g_0 = g_3$. The transcription rates are defined by

$$\omega_{gi}(g_j, a) = w_g \frac{a}{\theta_{\mathrm{nr}} + a} R(g_j), \qquad R(g) := \frac{1}{1 + \left({}^{g}/_{K_g}\right)^h}, \tag{52}$$

where $R(g)$ denotes the gene regulation function. The translation rates are defined analogously to (9) by

$$\nu_{gi}(c_{gi}, a) = c_{gi} \frac{\gamma(a)}{n_g}, \qquad i = \{1, 2, 3\}\,. \tag{53}$$

We include the additional consumption of energy and free ribosomes as:

$$\dot{a} = n_s \nu_{\mathrm{cat}}(e_m, s_i) - \lambda a - \sum_{\substack{x \in \\ \{r,t,m,q\}}} n_x \nu_x(c_x, a) \; - \sum_{i=\{1,2,3\}} n_g \nu_{gi}(c_{gi}, a),$$

$$\dot{r} = \nu_r(c_r, a) - \lambda r + \sum_{\substack{x \in \\ \{r,t,m,q\}}} (\nu_x(c_x, a) - k_b r m_x + k_u c_x) \tag{54}$$

$$+ \sum_{i=\{1,2,3\}} (\nu_{gi}(c_{gi}, a) - k_b r m_{gi} + k_u c_{gi}).$$

Finally, following Eq. 14 the growth rate becomes:

$$\lambda = \frac{\gamma(a)}{M} \left(\sum_{\substack{x \in \\ \{r,t,m,q\}}} c_x + \sum_{i=\{1,2,3\}} c_{gi} \right). \tag{55}$$

with the value of M unchanged.

Parameters: Transcript and protein half-lives were assumed to be two and four minutes, respectively [24], so that $d_{m,g} = {}^{\ln 2}/_{2}$ and $d_g = {}^{\ln 2}/_{4}$. The transcriptional parameters are: $K_g = 100$, $h = 2$ and $n_g = 300$ (equal to the length of the non-ribosomal proteins in Table S2). In all simulations we varied the induction level, w_g, across several orders of magnitude, and for Fig. 3C we varied the nutrient efficiency n_s.

S5.2 The isolated repressilator

We compared our host-aware repressilator with the standard model of an isolated repressilator [24]:

$$\dot{m}_{gi} = w_g R(g_{i-1}) - (d_{m,g} + \lambda_{\text{eff}}) m_{gi}, \qquad g_0 = g_3, \tag{56}$$

$$\dot{g}_i = k_{\text{eff}} m_{gi} - (d_g + \lambda_{\text{eff}}) g_i, \qquad i = \{1, 2, 3\}, \tag{57}$$

We used the same parameter values as the host-aware model. Additionally, we set the effective dilution rate, $\lambda_{\text{eff}} = 0.022$ min^{-1}, equal to the growth rate predicted by the model of the wild-type cell (without the synthetic circuit) for a nutrient efficiency of $n_s = 0.5$. We chose the effective translation rate, $k_{\text{eff}} = 0.6$ min^{-1}, so that the amplitudes of levels of repressors covered similar values as those in the host-aware model, at least for realistic value of $w_g < 10^3$mRNAs/ min, and varied the induction level within $w_g \in [1,\ 10^4]$.

S5.3 The isolated model ignores resource trade-offs

The host-aware and the isolated models show qualitatively different behaviours (Fig. 3c, main text), but less so in rich nutrient conditions (Fig. S3). While the repressilator proteins oscillate substantially, the other cellular components maintain relatively stable levels (Fig. S4). We conclude that the differences between the behaviours of the two models are because the isolated model ignores depletion of resources within the host cell.

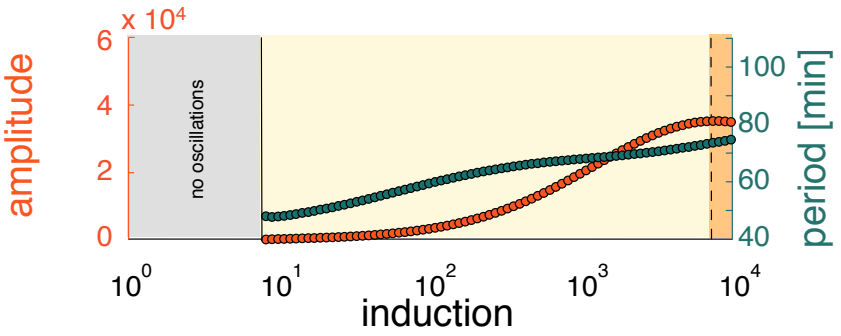

Figure S3: In rich conditions, the oscillations of the host-aware repressilator resemble those of the isolated repressilator (Fig. 3d, lower panel). Here, we used a high nutrient efficiency, $n_s = 15$ (cf. Fig. 3d in the main text with $n_s = 0.5$). The host over-loads only for unrealistically high induction ($w_g > 70000$ mRNAs/min), coinciding with a drop in the amplitude of oscillations. In the isolated repressilator, both period and amplitude grow with increasing induction.

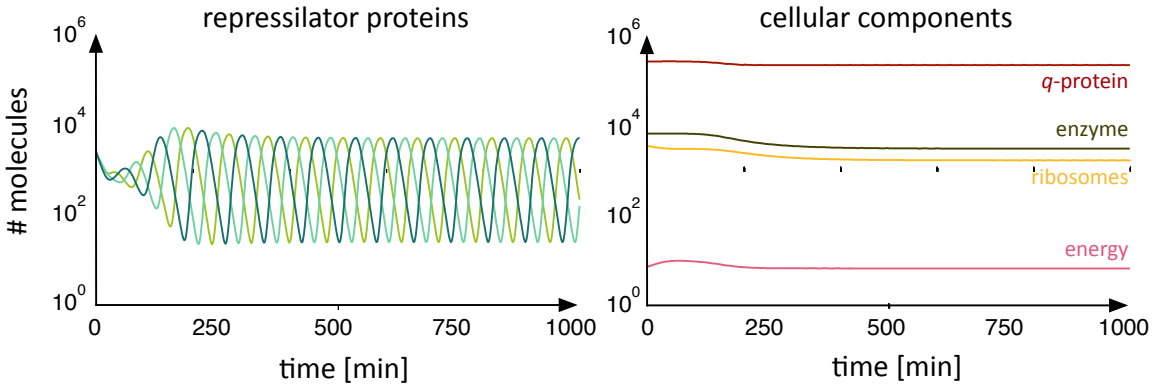

Figure S4: Oscillations in the repressilator proteins (left) barely affect the steady-state levels of other cellular components, which maintain stable levels (right). Here, $n_s = 0.5$, $s = 10\,000$ and the induction strength is $w_g = 614$ mRNAs/min), at which the amplitude of the oscillations is maximal (Fig. 3d).

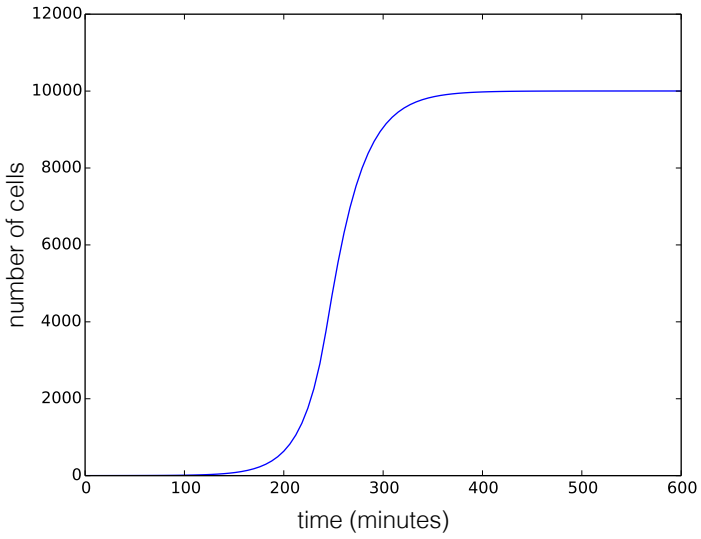

Figure S5: The multi-level model has a typical growth curve. We show the growth of a population of cells simulated using Eqs. (58) and (60) and the equations of Sec. S1 for all intracellular variables. Here we first simulated the intracellular reactions to steady-state with a fixed amount of extracellular nutrient to find suitable initial conditions. We then set the number of nutrient transporters to 1 (to give a lag) and simulated with an initial amount of 10^{10} nutrient molecules, which were not replenished. The population stopped growing shortly after extracellular nutrient was exhausted. Here $n_s = 100$ and $K_\gamma = 3.0 \times 10^8$.

S6 Multiscale simulations and population growth

S6.1 Including population growth

The growth of a homogenous population of cells can be straightforwardly included in our model. Assuming a death rate of individual cells of d_N, the total number of cells obeys

$$\dot{N} = \lambda N - d_N N \tag{58}$$

and grows exponentially if $\lambda > d_N$. For an intracellular molecule x, the total amount of x in the population, $X = xN$, obeys

$$\dot{X} = \lambda X - d_N X + \dot{x} N \tag{59}$$

using the chain rule. If the rate of change of intracellular molecules is zero, $\dot{x} = 0$, then the population is in exponential growth because all quantities at the population level grow exponentially, provided that $\lambda > d_N$.

To include the potential for competition between cells, we allow the external nutrient to change with time:

$$\dot{s} = k_{\text{in}} - \nu_{\text{imp}}(e_t, s)N - d_s s \tag{60}$$

with k_{in} being a constant rate of influx and d_s being a constant rate of efflux. To model growth in a chemostat, we would set $d_s = d_N$ with both equal to the chemostat's rate of dilution. All other quantities, all of which are intracellular, obey the equations given in Sec. S1. Fig. S5 shows a typical growth curve. The smoothness of the approach of N to its final value is greater if the nutrient quality n_s is large enough to allow the population to continue to grow using intracellular energy when extracellular nutrient is depleted.

If there is an influx of nutrient, the system goes to a steady-state with $\lambda = d_N$ from Eq. (58). If we consider the total amount of energy in the population either free or bound up in proteins, then its dynamics can be shown to obey

$$\frac{d}{dt}\left[N(M + n_s s_i + a) + n_s s\right] = n_s(k_{\text{in}} - d_s s) - d_N N(M + n_s s_i + a). \tag{61}$$

At steady-state, then

$$N = \frac{n_s(k_{\text{in}} - d_s s)}{d_N(M + n_s s_i + a)} \approx \frac{n_s k_{\text{in}}}{d_N M} \tag{62}$$

assuming $M \gg n_s s_i + a$ and $k_{\text{in}} \gg d_s s$ under steady-state conditions.

S6.2 Finding evolutionarily stable strategies

S6.2.1 Invasion analysis

Our goal is to study gene regulation by determining the evolutionarily stable value of the maximum rate of transcription of the enzymes ($w_e = w_t = w_m$ in Eq. (10)). To compete a resident strain and a mutant, we first find the steady-state conditions of the resident. We simulate a single cell in an environment with a fixed amount of

nutrient to determine initial conditions and then simulate the growth to steady-state of a population of cells starting from one cell with these initial conditions but now in an environment with a constant influx of nutrients. To determine if a mutant can outcompete the resident, we augment the system with differential equations describing the growth of the mutant population. The mutants have initial conditions identical to the steady-state conditions of the resident except for the mutated value of the trait (w_e) and an initial number of mutants 10^6 times smaller than the steady-state number of residents. The mutant and resident compete for the extracellular nutrient, and only the equation for the nutrient is affected by this competition:

$$\dot{s} = k_{\text{in}} - \nu_{\text{imp}}(e_t^{(r)}, s)N^{(r)} - \nu_{\text{imp}}(e_t^{(m)}, s)N^{(m)} - d_N s, \tag{63}$$

where superscripts indicate which population the variable belongs to, while the population sizes have dynamics according to Eq. (58):

$$\dot{N}^{(r)} = \lambda^{(r)} N^{(r)} - d_N N^{(r)}, \tag{64}$$

$$\dot{N}^{(r)} = \lambda^{(m)} N^{(m)} - d_N N^{(m)}. \tag{65}$$

When the augmented system has reached steady-state, we score the outcome of the competition by the steady-state fraction of mutants, ${}^{N_m}/_{N_r+N_m}$, which is one if the mutant invades completely and zero if the mutant goes extinct.

S6.2.2 Parameter values

Most parameter values are unchanged from Table S2 except $n_s = 100$ and $K_\gamma = 3.0 \times 10^8$. We set $d_s = d_N = 0.01$ min^{-1} in Eq. (58).

S6.2.3 Two extracellular nutrients

We consider a system that can metabolize two types of nutrient: s_a and s_b. The genome includes genes for a transporter and a metabolic enzyme for each nutrient, and expression of both these genes is identically and constitutively expressed, and so only depends on levels of energy. We fix w_b, the maximum transcription rate of the enzymes for s_b, but let w_a, the maximum transcription rate of the enzymes for s_a, evolve. Both nutrient systems have the same parameters except that the b nutrient is energetically richer than then a nutrient, $n_{s,b} = 100 n_{s,a}$. Each extracellular nutrient obeys an equation similar to Eq. (63), and we implemented the invasion analysis analogously to the single nutrient example (Sec. S6.2.1).

We can also derive an expression equivalent to Eq. (62). The total energy of the system is

$$N\left[M + \sum_k n_{s,k} s_{i,k} + a\right] + \sum_k n_{s,k} s_k, \tag{66}$$

where the sum is over both nutrients. Differentiating the total energy with respect to time and setting the result to zero (and imposing $\lambda = d_N$ from Eq. (58)), we find that

$$N = \frac{\sum_k n_{s,k}\left(k_{\text{in},k} - d_N s_k\right)}{d_N\left[M + \sum_k n_{s,k} s_{i,k} + a\right]} \tag{67}$$

at steady-state.

Supplementary References

[1] Taniguchi Y, *et al.* (2010) Quantifying e. coli proteome and transcriptome with single-molecule sensitivity in single cells. *Science* 329:533–538.

[2] Keseler IM, *et al.* (2011) Ecocyc: a comprehensive database of escherichia coli biology. *Nucleic Acids Research* 39:D583–D590.

[3] Brandt F, *et al.* (2009) The native 3D organization of bacterial polysomes. *Cell* 136:261–271.

[4] Bremer H, Dennis P (1996) Modulation of chemical composition and other parameters of the cell by growth rate. In Neidhardt C, ed., Escherichia coli *and* Salmonella (ASM Press, Washington, DC), pp. 1553–1569.

[5] Dornmair K, Overath P, Jähnig F (1989) Fast measurement of galactoside transport by lactose permease. *J Biol Chem* 264:342–346.

[6] Albe KR, Butler MH, Wright BE (1990) Cellular concentrations of enzymes and their substrates. *J Theor Biol* 143:163–195.

[7] Russell JB, Cook GM (1995) Energetics of bacterial growth: balance of anabolic and catabolic reactions. *Microbiol Rev* 59:48–62.

[8] Wagner A (2005) Energy constraints on the evolution of gene expression. *Mol Biol Evol* 22:1365–1374.

[9] Warner JR (1999) The economics of ribosome biosynthesis in yeast. *Trends Biochem Sci* 24:437–440.

[10] Cleland W (1975) Partition analysis and concept of net rate constants as tools in enzyme kinetics. *Biochemistry* 14:3220–3224.

[11] Klumpp S, Zhang Z, Hwa T (2009) Growth rate-dependent global effects on gene expression in bacteria. *Cell* 139:1366–1375.

[12] Ehrenberg M, Kurland C (1984) Costs of accuracy determined by a maximal growth rate constraint. *Q Rev Biophys* 17:45–82.

[13] Scott M, Gunderson CW, Mateescu EM, Zhang Z, Hwa T (2010) Interdependence of cell growth and gene expression: origins and consequences. *Science* 330:1099–1102.

[14] Scott M, Hwa T (2011) Bacterial growth laws and their applications. *Curr Opin Biotech* 22:559–565.

[15] Siso-Nadal F, Ollivier JF, Swain PS (2007) Facile: a command-line network compiler for systems biology. *BMC Syst Biol* 1:36.

[16] Monod J (1949) The Growth of Bacterial Cultures. *Ann Rev Microbiol* 3:371–394.

[17] Klumpp S, Scott M, Pedersen S, Hwa T (2013) Molecular crowding limits translation and cell growth. *Proc Nat Acad Sci USA* 110:16754–16759.

[18] Scott M, Klumpp S, Mateescu EM, Hwa T (2014) Emergence of robust growth laws from optimal regulation of ribosome synthesis. *Mol Syst Biol* 10:747–747.

[19] Haario H, Laine M, Mira A, Saksman E (2006) DRAM: efficient adaptive MCMC. *Stat and Comput* 16:339–354.

[20] Komorowski M, Costa MJ, Rand DA, Stumpf MP (2011) Sensitivity, robustness, and identifiability in stochastic chemical kinetics models. *Proc Nat Acad Sci USA* 108:8645–8650.

[21] Brown KS, Sethna JP (2003) Statistical mechanical approaches to models with many poorly known parameters. *Phys Rev E* 68:021904.

[22] Gutenkunst RN, *et al.* (2007) Universally sloppy parameter sensitivities in systems biology models. *PLoS Comput Biol* 3:e189.

[23] DeLuna A, Springer M, Kirschner MW, Kishony R (2010) Need-based up-regulation of protein levels in response to deletion of their duplicate genes. *PLoS Biol* 8:e1000347.

[24] Elowitz MB, Leibler S (2000) A synthetic oscillatory network of transcriptional regulators. *Nature* 403:335–338.